ORIGINAL PAPER

Relationship between SST anomalies and the intensity of intraseasonal variability

Fei Liu[1,2] · Lei Zhou[3] · Jian Ling[4] · Xiouhua Fu[5] · Gang Huang[4,6]

Abstract Intraseasonal variability (ISV) is a primary source for the sub-seasonal prediction that affects the livelihood of billions of people. Interannual variation of ISV intensity is important for seasonal prediction of ISV impacts on severe weathers. Existing measures of overall tropical ISV intensity, however, do not show any significant simultaneous relationship with external sea surface temperature anomalies (SSTAs). In this study, it is proposed that the ISV intensity, represented by the seasonal standard deviation of the 30–90-day filtered outgoing longwave radiation (OLR), has a good relation with the external SSTAs. With this measure, two major components of the interannual variability of global ISV intensity are detected for both boreal summer and winter: EOF1 calls its variability over the central Pacific and EOF2 is associated with the variability over the Indo-Pacific Warm Pool region.

More importantly, each of these two components is significantly related to SSTAs over a specific tropical region. The central Pacific ISV intensity is strong during central Pacific warming, while the ISV intensity is strong over the Indo-Pacific Warm Pool region during eastern Pacific cooling. The eastern and central Pacific warming has very different impacts on the ISV intensity: The eastern Pacific warming largely reduces the winter ISV intensity over the Indian Ocean, while the central Pacific warming only induces neutral winter ISV intensity anomalies over the Indian Ocean. In the summer, the ISV intensity variability is confined near the equator associated with the central Pacific warming; the eastern Pacific warming, however, induces large ISV intensity variability over the western North pacific because of strong northeastward propagation of the boreal summer ISV under the easterly vertical shear.

✉ Gang Huang
   hg@mail.iap.ac.cn

1   Earth System Modeling Center and Climate Dynamics Research
    Center, Nanjing University of Information Science and Technology,
    Nanjing 210024, China

2   Collaborative Innovation Center on Forecast and Evaluation of
    Meteorological Disasters, Nanjing University of Information Science
    and Technology, Nanjing 210044, China

3   State Key Lab of Satellite Ocean Environment Dynamics, Second
    Institute of Oceanography, Hangzhou, China

4   The State Key Laboratory of Numerical Modeling for Atmospheric
    Sciences and Geophysical Fluid Dynamics, Institute of Atmospheric
    Physics, Chinese Academy of sciences, Beijing 100029, China

5   International Pacific Research Center and Department of Meteorology,
    University of Hawaii at Manoa, Honolulu, HI 96822, USA

6   Joint Center for Global Change Studies (JCGCS), Beijing 100875,
    China

1 Introduction

Intraseasonal variability (ISV) with time scales of 30–90 days is an important mode in the tropical atmosphere, which exhibits strong multi-scale interaction (Wang and Liu 2011; Liu et al. 2012; Liu and Wang 2012a, 2013a) and prominent seasonal variation (Madden 1986; Wang and Rui 1990; Salby and Hendon 1994; Zhang and Dong 2004; Kikuchi et al. 2012). In the boreal winter, the dominant mode of ISV is the Madden-Julian Oscillation (MJO; Madden and Julian 1971, 1972) characterized by a planetary scale of wavenumbers 1–3, low frequency of 30–90 days, and a slow eastward propagation. In the boreal summer, the dominant boreal summer intraseasonal oscillation exhibits significant northward/northeastward propagation over the Indian Ocean (Yasunari 1979; Krishnamurti and Subrahmanyam 1982; Lau and Chan 1986; Annamalai and Sperber 2005; Wang et al. 2005) and northward/

northwestward propagation over the western North Pacific (Murakami 1984; Kemball-Cook and Wang 2001).

Although prevailing over the tropics at the intraseasonal time scale, the ISV has large impacts on a wide variety of climate phenomena across different spatial and temporal scales, such as the onsets and breaks of various monsoon systems (Yasunari 1979; Wang and Xie 1997; Martin and Schumacher 2011; Liu and Wang 2012b; Zhou and Murtugudde 2014), formation of tropical cyclones (Liebmann et al. 1994; Maloney and Hartmann 2000a, b; Serra et al. 2010), and other related climate anomalies (Zhang 2013). Further, the ISV also affects the onset of some El Niño events (Zhang 2005).

Due to the widespread impacts of the ISV on various weather and climate events, it is important to find out what controls the year-to-year variability of the ISV intensity. The ISV was found to exhibit a considerable interannual variation (Salby and Hendon 1994; Hendon et al. 1999; Slingo et al. 1999). There have been a few studies on the interannual variation of the ISV and its relationship with sea surface temperature anomalies (SSTAs), but the results remained controversial. Most studies demonstrated that the overall ISV intensity was uncorrelated with the SSTAs (Salby and Hendon 1994; Hendon et al. 1999; Slingo et al. 1999; Lawrence and Webster 2001). When using zonal mean 200-hPa zonal wind to measure the MJO intensity, a very weak linkage between the MJO intensity and SSTAs was found (Slingo et al. 1999). A weak relation between the MJO intensity and SSTAs was also reported by Hendon et al. (1999). The ISV intensity can be monitored by Wheeler-Hendon (WH) index (Wheeler and Hendon 2004; Hendon et al. 2007). When using the amplitude of the real-time multivariate MJO series 1 (RMM1) and 2 (RMM2), i.e., by summing the squares of RMM1 and RMM2 over the whole season, to represent the seasonal mean ISV strength, this WH intensity has no significant correlation with the SSTA over the Pacific (Fig. 1).

In the WH index, the RMM1 and RMM2 are associated with the convection anomalies of the ISV over the Maritime Continent and over the Pacific Ocean, respectively (Wheeler and Hendon 2004). The WH intensities representing by the seasonal mean standard deviation of RMM1 and RMM2 show the region-dependent ISV intensity. Similar results, as in Fig. 1, have been obtained (figure not shown). In the winter, both the WH intensity over the Maritime Continent (representing by RMM1) and over the Pacific Ocean (representing by RMM2) do not have significant correlation with the SSTA. In the summer, the WH intensity over the Maritime Continent is significantly correlated to the local SSTA over the Maritime Continent and the SSTA over the equatorial Atlantic; no significant correlation, however, has been found over the Pacific. The summer WH intensity over the Pacific also has no significant correlation with the global SSTA. These results show that the overall WH intensity and the region-dependent WH intensity all have no significant correlation with the equatorial Pacific SSTA associated with the El Niño-Southern Oscillation (ENSO).

Since the ENSO is the most energetic and predictable mode on the interannual time scale, the relation between the ISV intensity and ENSO has been extensively studied (Lau and Chan 1988; Lau and Shen 1988; Weickmann 1991; Takayabu et al. 1999; Kessler and Kleeman 2000; Bergman et al. 2001; Zhang and Gottschalck 2002; Teng and Wang 2003; Hendon et al. 2007; Yun et al. 2008); large discrepancies, however, exists for this relation. Some studies suggested that the overall amplitude of the ISV intensity has no relation with the ENSO (Hendon et al. 1999; Slingo et al. 1999), and the model calculations show very little interannual predictability of the ISV intensity (Waliser et al. 2001). In theory, however, the warm SST should enhance the deep convection of the MJO (Salby et al. 1994). Thus, during La Niña conditions, the MJO is mostly confined west of the date line, with largest activity located over the Indian Ocean and the western Pacific. In warm El Niño conditions, the convective anomalies associated with the oscillation appear to penetrate farther into the central pacific (Gualdi et al. 1999; Moon et al. 2011). The MJO strength in the western Pacific was correlated to the eastward extension of the Warm Pool's eastern edge (Anyamba and Weare 1995; Hendon et al. 1999; Kessler 2001), the increased ISV activity over the central Pacific during El Niño event was found (Liess et al. 2004), and the MJO activity over the equatorial Pacific from 160° E to the coast of South America is highly correlated to the collocated SSTAs (Fink and Speth 1997). Teng and Wang (2003) found that the relation between ISV and ENSO is seasonally and regionally dependent; the wintertime MJO is uncorrelated with the ENSO, but the boreal summer ISV in May–July is intensified during El Niño developing years. In the models, the leading empirical orthogonal function (EOF) modes of boreal summer ISV intensity are closely linked to the models' ENSO, which resembles the observed boreal summer ISV and ENSO relationship (Kim et al. 2008).

The unresolved issue is why the current measures of overall ISV intensity, such as the WH intensity and Slingo et al. index, show weak linkage between ISV intensity and SSTAs. A more general question is whether SSTAs affect the ISV. If they do, to what extent is the ISV determined by SSTAs and how? These questions call for a re-examination of the relationship between the ISV and the SSTAs.

2 Data

The outgoing longwave radiation (OLR) has also been widely used as a primary variable in the development of indices for the MJO (Waliser et al. 1999; Lo and Hendon 2000; Wheeler and Hendon 2004) and for the boreal summer ISV (Lee et al.
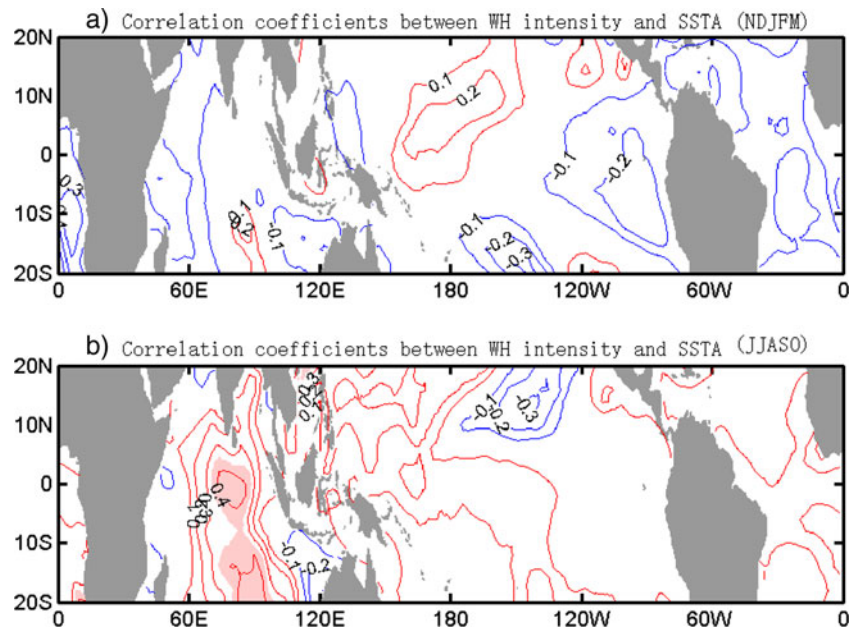
2013). We use the seasonal standard deviation of 30–90-day filtered OLR to represent the ISV intensity in this study.

The data sets used include the 30-year (1981–2010) daily advanced very high-resolution radiometer (AVHRR) OLR with 2.5° horizontal resolution based on the National Oceanic and Atmospheric Administration (NOAA) polar orbiting satellites (Liebmann and Smith 1996), the monthly mean winds and specific humidity at 850 hPa from the NCEP/Department of Energy (DOE) Reanalysis II (Kanamitsu et al. 2002) with 2.5° horizontal resolution, and the monthly mean SST from the Improved Extended Reconstructed SST (ERSST.v3b) data set developed by the NOAA (Smith et al. 2008) with 2° horizontal resolution. The period of June–October is selected to represent the boreal summer (Kikuchi et al. 2012; Lee et al. 2013). The period of November–March is selected to represent the boreal winter and the extended Australian summer season (Hendon et al. 1999).
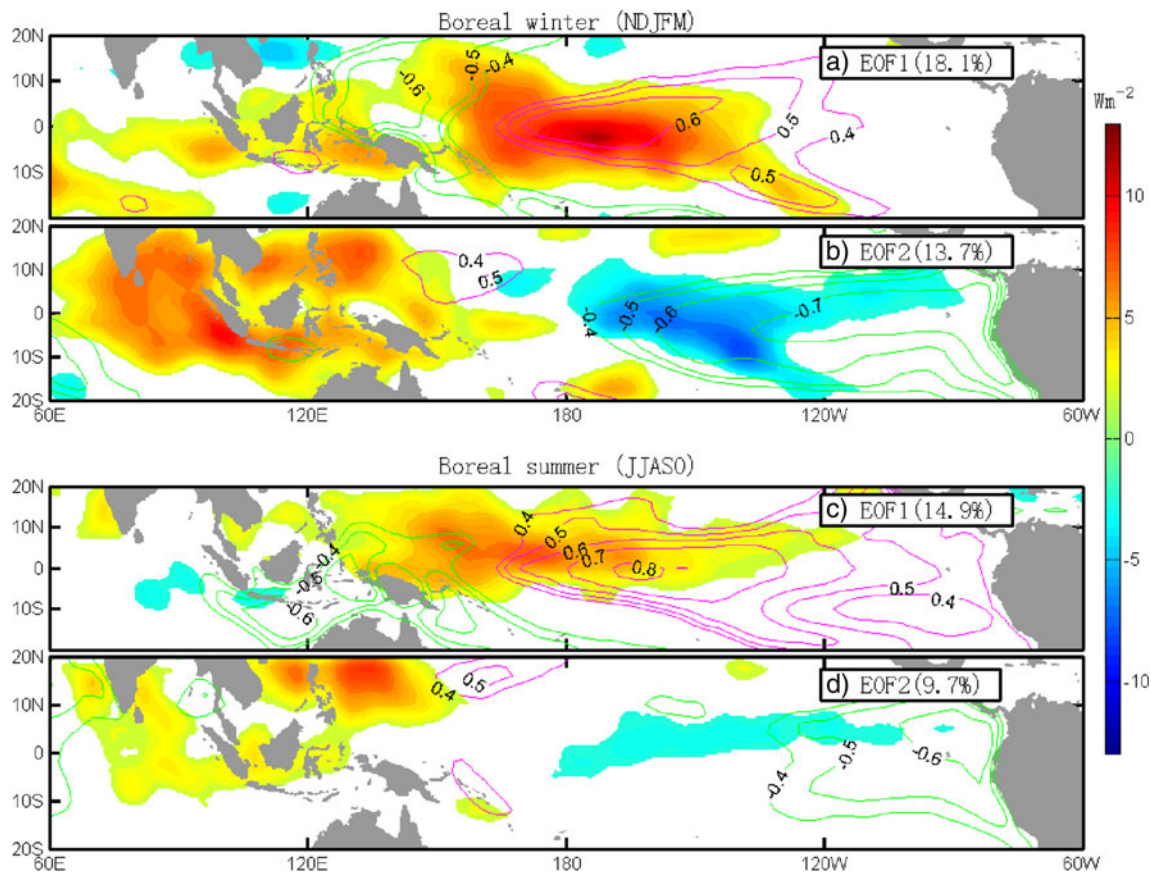
3 Interannual variability of ISV intensity and their SST control

In order to find out what controls the interannual variability of ISV intensity, a clear picture of the year-to-year variation of ISV intensity has to be obtained and we prefer using the EOF analysis. The climatological ISV intensity at each grid is obtained for the boreal summer and winter separately with the 30-year average (from 1981 to 2010) and is then removed from the total ISV intensity. In this work, only the ISV intensity within the tropical (20° S–20° N) channel is analyzed. The spatial structures of the two leading EOFs of ISV intensity are presented in Fig. 2. The percentage variance accounted for by

each EOF mode is 18.1 and 13.7 % for boreal winter and is 14.9 and 9.7 % for boreal summer. Thus, the first two leading EOF modes can account for 31.8 % (24.6 %) of total variance in the boreal winter (summer) tropics. They are well separated from the EOF3 (explains only 6.3 %) for winter, but not well separated for summer (explains only 6.4 %) based on the criteria of North et al. (North et al. 1982). Hence, we mainly focus on the first two EOFs.

In the winter, the variability of EOF1 is mainly located over the central Pacific region (Fig. 2a). The EOF2, however, is dominated by a strong variability in the Indo-Pacific Warm Pool region (Fig. 2b), although an out-of-phase variability is located over the eastern South Pacific. This means that the interannual variability of the boreal winter ISV intensity can be separated into two different components, which capture the ISV intensity over the central Pacific and Indo-Pacific Warm Pool regions, respectively. In the summer, the boreal summer ISV intensity can also be separated into two different components: The variability of EOF1 is mainly located over the central Pacific (Fig. 2c), and the EOF2 is dominated by a strong variability in the western North Pacific (Fig. 2d).

The simultaneous correlation maps between the SSTAs and each PC of the ISV intensity components are also superimposed in Fig. 2. Note that both components are significantly correlated to the seasonal mean SSTA for both seasons: EOF1 is related to the central Pacific SSTA (Fig. 2a, c), while EOF2 is related to the eastern Pacific SSTA (Fig. 2b, d). The highest correlation coefficients exceed 0.65 (above the 99 % confidence level) for both EOFs and both seasons, which means that these two EOFs are related to the central or eastern Pacific SSTA associated with the developing, developed, or decaying phase of the ENSO or associated with different types of the ENSO, i.e., the eastern Pacific

Fig. 2 Two major components of ISV intensity variability and their relationship with seasonal mean SSTA. *Shadings* denote spatial patterns of the first two EOFs of **a**, **b** boreal winter (November–March) ISV and **c**, **d** boreal summer (June–October) ISV intensity. The ISV intensity is represented by the seasonal standard deviation of 30–90-day band-pass filtered OLR. *Contours* denote simultaneous correlation coefficients between the seasonal mean SSTA and each PC of first two EOFs. *Purple* (*green*) contours denote positive (negative) correlation, and they are all significant ($r=0.36$) above the 95 % confidence level. For clarity of presentation, only ISV intensity with amplitude above 3 W m^{-2} is shaded

ENSO and the central Pacific ENSO. Strikingly, the relationship between these two components and the SSTA are out of phase in the tropical Pacific: EOF1 has a positive correlation with the central Pacific SSTA, while EOF2 has a negative correlation with the eastern Pacific SSTA. This out-of-phase relationship may explain why the overall tropical ISV intensity, the WH intensity that represents the global ISV intensity, has no significant correlation with seasonal mean SSTAs.

The physical processes behind SSTA controlling of these two ISV intensity components are discussed with the help of Fig. 3, which shows the regressed boreal winter anomalies of some fields with respect to each PC of the two ISV intensity EOFs. To compare with PC1 (Fig. 3a, c) more easily, the regressed maps with respect to –PC2 are given (Fig. 3b, d), so the regressed SSTAs over the central to eastern Pacific are both positive.

Before discussing how SSTA controls the ISV intensity, existing mechanisms should be mentioned first. Generally speaking, the rich moisture supply usually favors the growth of the ISV (Li and Wang 1994; Zhang 2005). The positive zonal moisture gradient also favors the growth of the ISV

(Maloney et al. 2010). The air–sea interaction is positive over low-level westerly wind for the ISV, and the evaporation feedback is negative for the ISV under the seasonal mean easterly wind (Emanuel 1987; Wang 1988; Wang and Xie 1998; Liu and Wang 2013b). The enhanced preceding ISV over the western Pacific will enhance the downstream out-of-phase ISV over the Indian Ocean through moisture and temperature advection (Zhao et al. 2013). In the boreal summer, the strong easterly vertical shear favors the northward propagation of the ISV (Jiang et al. 2004), and the ISV is enhanced over the western North Pacific (Liu and Wang 2014). In the year when these feedbacks are positive, the ISV is much active; thus, on the interannual time scale, the ISV intensity is strong compared to neutral years.

We first discuss the boreal winter ISV. During the years when the ISV intensity over the central Pacific is strong (Fig. 3a), there is a warming in the central Pacific, with positive seasonal mean moisture anomalies and strong low-level westerly wind anomalies located over the central Pacific. In the Indo-Pacific Warm Pool region, the moisture anomalies are negative, and they are accompanied by low-level easterly
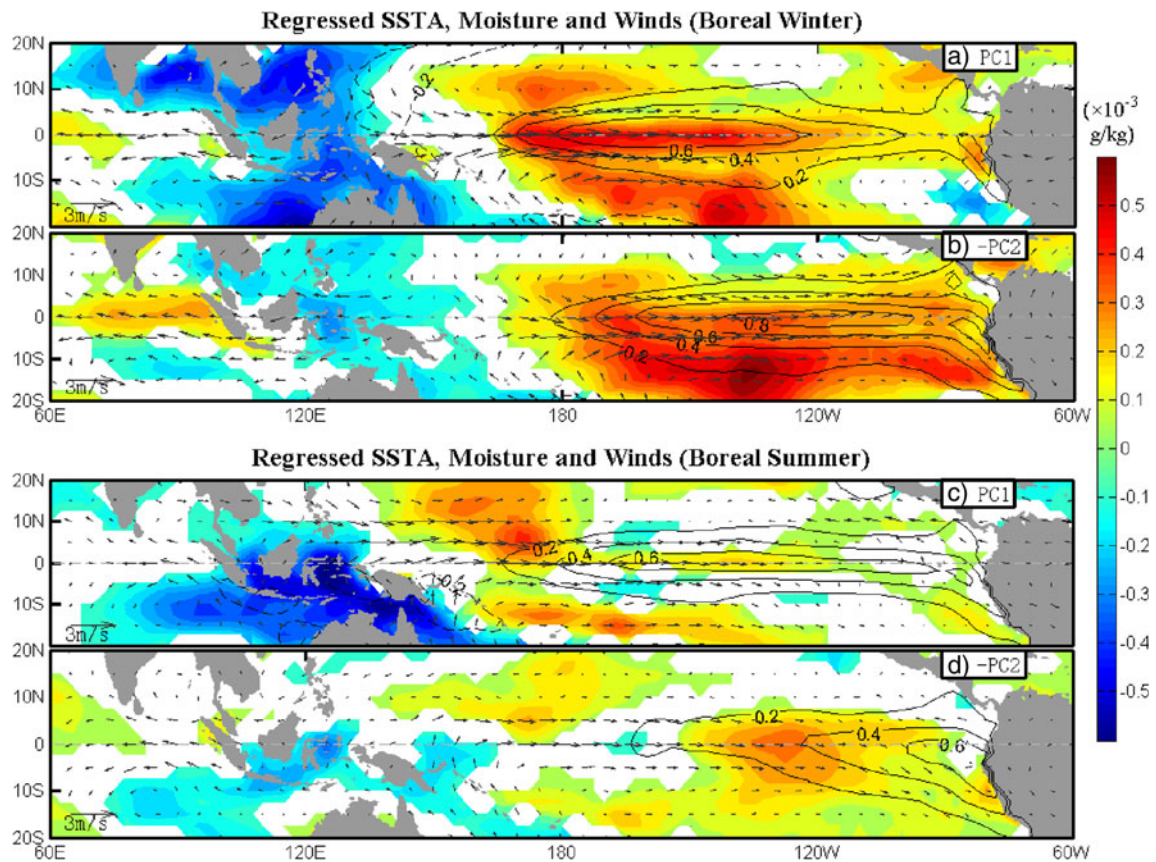
Fig. 3 Anomalies of seasonal mean state associated with the first two EOFs. Shown are regressed seasonal mean SSTA (*contours*; in °C), 850-hPa specific humidity anomalies (*shadings*; g kg^{-1}), and 850-hPa wind anomalies (*vectors*) of each of the first two PCs for **a**, **b** the boreal winter ISV and **c**, **d** the boreal summer ISV

wind anomalies. Over the central Pacific, the rich moisture supply favors the growth of the ISV (Zhang 2005). Under the seasonal mean low-level easterly wind, the air–sea interaction is a negative feedback for the ISV because the ISV easterly wind anomalies will cool down the SST in front of the ISV through increasing the evaporation and oceanic entrainment, and the cold SST will suppress the ISV (Wang and Xie 1998; Liu and Wang 2013b). Thus, the low-level westerly wind anomalies will reduce the climatological easterly wind in the central Pacific and suppress this negative feedback. As a result, the ISV is enhanced over the central Pacific. Over the Indo-Pacific Warm Pool, although the seasonal mean moisture anomalies are negative, anomalies of seasonal mean zonal moisture gradient are positive, and the zonal moisture advection favors the growth of the ISV (Maloney et al. 2010); thus, the ISV still can grow there (Fig. 2a).

In the years when the boreal winter ISV intensity over the Indo-Pacific Warm Pool is weak (Fig. 3b), positive SSTA occurs over the eastern Pacific, and positive seasonal mean moisture anomalies are located over the eastern South Pacific. Due to this eastern Pacific warming associated with the El Niño, the Walker circulation anomaly is reversed; thus, negative seasonal mean moisture anomalies and low-level

easterly wind anomalies appear in the Indo-Pacific Warm Pool region. Although the seasonal mean moisture is enhanced over the eastern South Pacific, the climatological mean moisture there is too low, and the ISV cannot be enhanced much (Fig. 2b). In the Indo-Pacific Warm Pool region, the negative mean moisture anomalies and low-level easterly winds are not favorable to the ISV. Meanwhile, the anomalies of seasonal mean zonal moisture gradient are also weak because the moisture anomalies in the eastern South Pacific are too far away. The ISV thus is much suppressed in the Indo-Pacific Warm Pool region. Conversely, the ISV is very strong in the Indo-Pacific Warm Pool region due to the eastern Pacific cooling.

In boreal summer, similar processes also exist (Fig. 3c, d). The EOF1 is more like the ENSO-related ISV mode in the observation (Teng and Wang 2003) and in the models (Kim et al. 2008), and the strong easterly vertical shear related to the El Niño is favorable for the growth of the ISV. Because of strong northward propagation of the ISV, the strong variations are observed over the western North Pacific (Fig. 2d).

Although the anomalous moisture and low-level flow patterns are generally similar over the Indian Ocean in the winter (Fig. 3a, b), the ISV intensity is almost neutral over the Indian

Ocean associated with the central Pacific warming (Fig. 2a), while it is much reduced associated with the eastern pacific warming (Fig. 2b). This difference is induced by different mean states over the western Pacific. When the central Pacific is warm, the ISV is much enhanced over the western Pacific (Fig. 2a) because of the positive zonal moisture gradient and low tropospheric westerly (Maloney 2009; Liu and Wang 2013b). The easterly wind anomalies of the downstream Rossby waves response to a preceding suppressed phase ISV over the western Pacific usually increase the moisture and temperature anomalies over the western Indian Ocean and initiate the ISV there (Zhao et al. 2013), and the enhanced preceding ISV over the western Pacific will also enhance the downstream out-of-phase ISV over the Indian Ocean. This positive feedback will compete against the negative feedback of the Indian Ocean mean states and produce a neutral variation of the ISV intensity over the Indian Ocean. When the eastern Pacific is warm, the positive seasonal mean moisture and low-level westerly winds are far away from the western Pacific (Fig. 3b). The ISV cannot be enhanced over the western Pacific, and the positive feedback of the preceding ISV disappears over the Indian Ocean; thus, the ISV over the Indian Ocean will be largely reduced by the negative feedback of the Indian Ocean mean states.

In the summer, although the easterly vertical wind shear plays a critical role in regulating the northward propagation of the boreal summer ISV, the ISV intensity of EOF1 is more near the equator (Fig. 2c), while the ISV intensity of EOF2 is largely off-equator (Fig. 2d). This is because the strong climatological mean *easterly* vertical shear with a magnitude of 25 m/s exists over the Indian Ocean and western North Pacific, while strong climatological mean *westerly* vertical shear with a magnitude of 15 m/s exists over the central North Pacific (Teng and Wang 2003). When the eastern Pacific is cold, the easterly vertical shear still exists over the Indian Ocean and western North

Pacific, and the enhanced boreal summer ISV can propagate northeastward to the western North Pacific. When the central Pacific is warm, over the central North Pacific the westerly vertical shear still prevails, and the northward propagation disappears and the enhanced boreal summer ISV is confined near the equator. Thus, these two EOFs show ISV intensity near and off the equator respectively. Keep in mind that we are focusing on the anomalous ISV. When the central Pacific is warm, the northwestward propagation of ISV still exists over the western North Pacific. This western North Pacific ISV, however, is not stronger than that of neutral years because the enhanced ISV is located over the central Pacific.

For both seasons, there is a phase lag between the Pacific warming related to these two EOF modes (Fig. 3). We conclude that it is this phase lag that controls these different ISV intensity–SSTA relationships. When the SST warming occurs in the central Pacific, the associated rich moisture and low-level westerly wind anomalies or easterly vertical shear favor the growth of the ISV over the central Pacific. When the SSTA occurs in the eastern Pacific, the ISV convection cannot be enhanced there because of the low climatological SST there. The Indo-Pacific Warm Pool region, however, is strongly impacted by the eastern Pacific SSTA through the Walker circulation, and the seasonal mean moisture anomalies affected by the eastern Pacific SSTA will control the strength of ISV in the Indo-Pacific Warm Pool region.

4 Concluding remarks

In this paper, we show that the two major components of ISV intensity variability, namely EOF1 associated with the central Pacific variability and EOF2 associated with the Indo-Pacific Warm Pool variability, are highly controlled by the SSTA

Fig. 4 Relationship between two components of ISV intensity variability and WH intensity. PC1 (*red dashed curve*), PC2 (*blue dashed curve*) associated with the first two EOFs in Fig. 2, and WH intensity (*black curve*) are drawn for the **a** boreal winter ISV and **b** boreal summer ISV. The correlation between WH intensity and PC1 (WH intensity and PC2) is 0.53 (0.63) for the boreal winter ISV and is 0.41 (0.45) for the boreal summer ISV
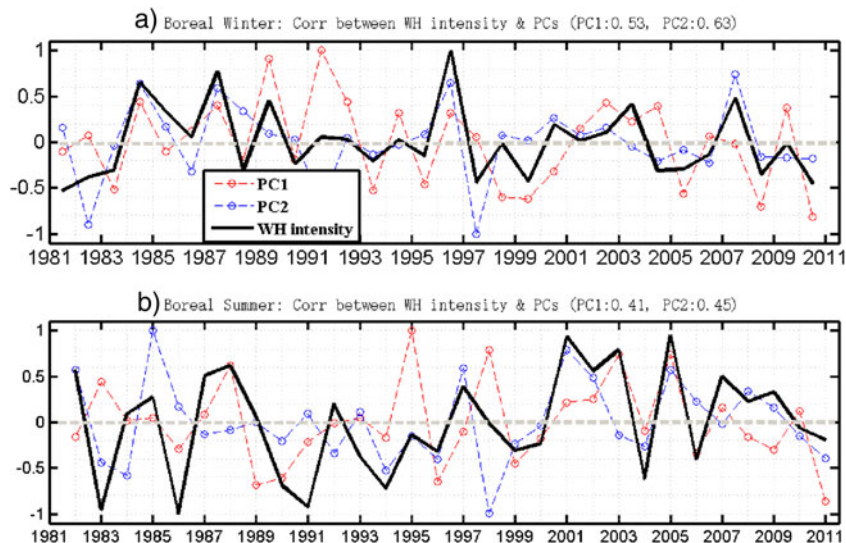
forcing for both the boreal winter and boreal summer ISV intensity (Figs. 2 and 3).

Although local SST increase will enhance the ISV intensity by increasing convection (Salby et al. 1994), the seasonal mean zonal moisture gradient (Maloney 2009), zonal winds induced evaporation (Emanuel 1987; Wang 1988), and the preceding ISV induced ISV initiation at the western Indian Ocean (Zhao et al. 2013) all can affect the ISV intensity. Thus, the central and eastern Pacific warming induces very different ISV intensity patterns. The *eastern* Pacific warming largely reduces the winter ISV intensity over the Indian Ocean, while neutral winter ISV intensity is induced over the Indian Ocean by the *central* Pacific warming. In the summer, the ISV intensity variability is confined near the equator associated with the central Pacific warming; the eastern Pacific warming, however, induces large ISV intensity variability over the western North pacific because of strong northeastward propagation of the boreal summer ISV under the easterly vertical shear over the Indo-Pacific Warm Pool region.

Since EOF1 and EOF2 are the two major components of the interannual variability of global ISV intensity and account for about 30 % of the total variance, do they have any relationship with the overall tropical ISV intensity, such as the WH intensity? We checked the relationship between each of these two EOFs and the WH intensity that is represented by the seasonal mean amplitude of the WH index RMM1 and RMM2 (Hendon et al. 2007). Figure 4 shows that each of these two components has a significant (above 99 % confidence level) positive correlation with the WH intensity for both seasons. Since these two components have out-of-phase correlations with the SSTA over the Pacific (Fig. 2), the sum of them only gives a weak correlation with the SSTA in the Pacific (not shown). This explains why the WH intensity has no significant correlation with the SSTA because it is more like the sum of these two separated components.

The OLR, representing the convective anomaly, prevails in the eastern Hemisphere; the circulation anomaly, however, is not confined to the eastern Hemisphere (Hendon and Salby 1994; Adames and Wallace 2014). In recent works (Kiladis et al. 2014), the more local and convection based, the more will the index of ISV be influenced by the SSTA. In this work, we use the OLR to measure the ISV intensity, which may overemphasize the local stationary oscillation. To better compare with the Slingo's index or WH index, the circulation anomaly of the ISV propagating around the globe should be further studied in the future works.

In this work, we studied the direct relationship between the ISV intensity and SSTAs rather than the ISV intensity–ENSO relationship. The complicated relationship between the ISV intensity and different phases and different types of ENSO should be discussed in the following works. Since each of these two major components is well determined by the SSTA forcing, the seasonal prediction of ISV intensity can be made using an empirical model, which is also our ongoing research.

References

Adames ÁF, Wallace JM (2014) Three-dimensional structure and evolution of the vertical velocity and divergence fields in the MJO. J Atmos Sci 71:4661–4681

Annamalai H, Sperber K (2005) Regional heat sources and the active and break phases of boreal summer intraseasonal (30-50 day) variability*. J Atmos Sci 62:2726–2748

Anyamba EK, Weare BC (1995) Temporal variability of the 40 50-day oscillation in tropical convection. Int J Climatol 15:379–402

Bergman JW, Hendon HH, Weickmann KM (2001) Intraseasonal air-sea interactions at the onset of El Nino. J Clim 14:1702–1719

Emanuel KA (1987) An air-sea interaction model of intraseasonal oscillations in the tropics. J Atmos Sci 44:2324–2340

Fink A, Speth P (1997) Some potential forcing mechanisms of the year-to-year variability of the tropical convection and its intraseasonal (25–70-day) variability. Int J Climatol 17:1513–1534

Gualdi S, Navarra A, Tinarelli G (1999) The interannual variability of the Madden–Julian oscillation in an ensemble of GCM simulations. Clim Dynam 15:643–658

Hendon HH, Salby ML (1994) The life cycle of the Madden-Julian oscillation. J Atmos Sci 51:2225–2237

Hendon HH, Zhang C, Glick JD (1999) Interannual variation of the Madden-Julian Oscillation during austral summer. J Clim 12:2538–2550

Hendon HH, Wheeler MC, Zhang C (2007) Seasonal dependence of the MJO-ENSO relationship. J Clim 20:531–543

Jiang X, Li T, Wang B (2004) Structures and mechanisms of the northward propagating boreal summer intraseasonal oscillation*. J Clim 17:1022–1039

Kanamitsu M, Ebisuzaki W, Woollen J, Yang S-K, Hnilo J, Fiorino M, Potter G (2002) NCEP-DOE AMIP-II reanalysis (R-2). B Am Meteorol Soc 83:1631–1643

Kemball-Cook S, Wang B (2001) Equatorial waves and air-sea interaction in the boreal summer intraseasonal oscillation. J Clim 14:2923–2942

Kessler WS (2001) EOF representations of the Madden-Julian oscillation and its connection with ENSO*. J Clim 14:3055–3061

Kessler WS, Kleeman R (2000) Rectification of the Madden-Julian oscillation into the ENSO cycle. J Clim 13:3560–3575

Kikuchi K, Wang B, Kajikawa Y (2012) Bimodal representation of the tropical intraseasonal oscillation. Clim Dynam 38:1989–2000

Kiladis GN et al (2014) A comparison of OLR and circulation-based indices for tracking the MJO. Mon Weather Rev 142:1697–1715

Kim H-M, Kang I-S, Wang B, Lee J-Y (2008) Interannual variations of the boreal summer intraseasonal variability predicted by ten atmosphere–ocean coupled models. Clim Dynam 30:485–496

Krishnamurti TN, Subrahmanyam D (1982) The 30-50 day mode at 850 mb during MONEX. J Atmos Sci 39:2088–2095

Lau K-M, Chan P (1986) Aspects of the 40-50 day oscillation during the northern summer as inferred from outgoing longwave radiation. Mon Weather Rev 114:1354–1367

Lau K-M, Chan PH (1988) Intraseasonal and interannual variations of tropical convection: a possible link between the 40-50 day oscillation and ENSO? J Atmos Sci 45:506–521

Lau K, Shen S (1988) On the dynamics of intraseasonal oscillations and ENSO. J Atmos Sci 45:1781–1797

Lawrence DM, Webster PJ (2001) Interannual variations of the intraseasonal oscillation in the south Asian summer monsoon region. J Clim 14:2910–2922

Lee J-Y, Wang B, Wheeler MC, Fu X, Waliser DE, Kang I-S (2013) Real-time multivariate indices for the boreal summer intraseasonal oscillation over the Asian summer monsoon region. Clim Dynam 40: 493–509

Li T, Wang B (1994) The influence of sea surface temperature on the tropical intraseasonal oscillation: a numerical study. Mon Weather Rev 122:2349–2362

Liebmann B, Smith CA (1996) Description of a complete (interpolated) outgoing longwave radiation dataset. Bull Am Meteorol Soc 77: 1275–1277

Liebmann B, Hendon HH, Glick JD (1994) The relationship between tropical cyclones of the western Pacific and Indian oceans and the Madden-Julian oscillation. J Meteorol Soc Jpn 72:401–412

Liess S, Bengtsson L, Arpe K (2004) The intraseasonal oscillation in ECHAM4 Part I: coupled to a comprehensive ocean model. Clim Dynam 22:653–669

Liu F, Wang B (2012a) A model for the interaction between 2-day waves and moist Kelvin waves*. J Atmos Sci 69:611–625

Liu F, Wang B (2012b) A conceptual model for self-sustained active-break Indian summer monsoon. Geophys Res Lett 39, L20814

Liu F, Wang B (2013a) Impacts of upscale heat and momentum transfer by moist Kelvin waves on the Madden–Julian oscillation: a theoretical model study. Clim Dynam 40:213–224

Liu F, Wang B (2013b) An air–sea coupled skeleton model for the Madden–Julian oscillation*. J Atmos Sci 70:3147–3156

Liu F, Wang B (2014) A mechanism for explaining the maximum intraseasonal oscillation center over the Western North Pacific*. J Clim 27:958–968

Liu F, Huang G, Feng L (2012) Critical roles of convective momentum transfer in sustaining the multi-scale Madden–Julian oscillation. Theor Appl Climatol 108:471–477

Lo F, Hendon HH (2000) Empirical extended-range prediction of the Madden-Julian oscillation. Mon Weather Rev 128:2528–2543

Madden RA (1986) Seasonal variations of the 40-50 day oscillation in the tropics. J Atmos Sci 43:3138–3158

Madden RA, Julian PR (1971) Detection of a 40-50 day oscillation in the zonal wind in the tropical Pacific. J Atmos Sci 28:702–708

Madden RA, Julian PR (1972) Description of global-scale circulation cells in the tropics with a 40-50 day period. J Atmos Sci 29:1109–1123

Maloney ED (2009) The moist static energy budget of a composite tropical intraseasonal oscillation in a climate model. J Clim 22:711–729

Maloney ED, Hartmann DL (2000a) Modulation of hurricane activity in the Gulf of Mexico by the Madden-Julian oscillation. Science 287: 2002–2004

Maloney ED, Hartmann DL (2000b) Modulation of Eastern North Pacific hurricanes by the Madden-Julian oscillation. J Clim 13:1451–1460

Maloney ED, Sobel AH, Hannah WM (2010) Intraseasonal variability in an aquaplanet general circulation model. J Adv Model Earth Syst 2:1–14

Martin ER, Schumacher C (2011) The Caribbean low-level jet and its relationship with precipitation in IPCC AR4 models. J Clim 24: 5935–5950

Moon J-Y, Wang B, Ha K-J (2011) ENSO regulation of MJO teleconnection. Clim Dynam 37:1133–1149

Murakami M (1984) Analysis of the deep convective activity over the Western Pacific and Southeast Asia. II: seasonal and intraseasonal variations during Northern Summer. J Meteorol Soc Jpn 62:88–108

North GR, Bell TL, Cahalan RF, Moeng FJ (1982) Sampling errors in the estimation of empirical orthogonal functions. Mon Weather Rev 110:699–706

Salby ML, Hendon HH (1994) Intraseasonal behavior of clouds, temperature, and motion in the Tropics. J Atmos Sci 51:2207–2224

Salby ML, Garcia RR, Hendon HH (1994) Planetary-scale circulations in the presence of climatological and wave-induced heating. J Atmos Sci 51:2344–2367

Serra YL, Kiladis GN, Hodges KI (2010) Tracking and mean structure of easterly waves over the intra-Americas sea. J Clim 23:4823–4840

Slingo J, Rowell D, Sperber K, Nortley F (1999) On the predictability of the interannual behaviour of the Madden-Julian Oscillation and its relationship with El Niño. Q J Roy Meteor Soc 125:583–609

Smith TM, Reynolds RW, Peterson TC, Lawrimore J (2008) Improvements to NOAA's historical merged land-ocean surface temperature analysis (1880-2006). J Clim 21:2283–2296

Takayabu YN, Iguchi T, Kachi M, Shibata A, Kanzawa H (1999) Abrupt termination of the 1997–98 El Nino in response to a Madden–Julian oscillation. Nature 402:279–282

Teng H, Wang B (2003) Interannual variations of the boreal summer intraseasonal oscillation in the Asian-Pacific Region*. J Clim 16: 3572–3584

Waliser DE, Jones C, Schemm J-KE, Graham NE (1999) A statistical extended-range tropical forecast model based on the slow evolution of the Madden-Julian Oscillation. J Clim 12:1918–1939

Waliser DE, Zhang Z, Lau K, Kim J-H (2001) Interannual sea surface temperature variability and the predictability of tropical intraseasonal variability. J Atmos Sci 58:2596–2615

Wang B (1988) Comments on "An air-sea interaction model of intraseasonal oscillation in the tropics". J Atmos Sci 45:3521–3525

Wang B, Liu F (2011) A model for scale interaction in the Madden-Julian oscillation*. J Atmospheric Sci 68:2524–2536

Wang B, Rui H (1990) Dynamics of the coupled moist Kelvin-Rossby wave on an equatorial β-plane. J Atmos Sci 47:397–413

Wang B, Xie X (1997) A model for the boreal summer intraseasonal oscillation. J Atmos Sci 54:72–86

Wang B, Xie X (1998) Coupled modes of the warm pool climate system. Part I: the role of air-sea interaction in maintaining Madden-Julian oscillation. J Clim 11:2116–2135

Wang B, Webster PJ, Teng H (2005) Antecedents and self-induction of active-break south Asian monsoon unraveled by satellites. Geophys Res Lett 32:4704

Weickmann K (1991) El Niño/Southern Oscillation and Madden-Julian (30–60 day) oscillations during 1981–1982. J Geophys Res: Oceans (1978–2012) 96:3187–3195

Wheeler MC, Hendon HH (2004) An all-season real-time multivariate MJO index: development of an index for monitoring and prediction. Mon Weather Rev 132:1917–1932

Yasunari T (1979) Cloudiness fluctuations associated with the Northern Hemisphere summer monsoon. J Meteor Soc Japan 57:227–242

Yun K-S, Seo K-H, Ha K-J (2008) Relationship between ENSO and northward propagating intraseasonal oscillation in the east Asian summer monsoon system. J Geophys Res 113, D14120

Zhang C (2005) Madden-Julian Oscillation. Rev Geophys 42:G2003

Zhang C (2013) Madden-Julian oscillation: bridging weather and climate. B Am Meteorol Soc 94:1849–1870

Zhang C, Dong M (2004) Seasonality in the Madden-Julian oscillation. J Clim 17:3169–3180

Zhang C, Gottschalck J (2002) SST anomalies of ENSO and the Madden-Julian oscillation in the equatorial Pacific. J Clim 15:2429–2445

Zhao C, Li T, Zhou T (2013) Precursor signals and processes associated with MJO initiation over the tropical Indian Ocean*. J Clim 26:291–307

Zhou L, Murtugudde R (2014) Impact of northward-propagating intraseasonal variability on the onset of Indian summer monsoon. J Clim 27:126–139